ISBN: 978-3-95450-214-1 ISSN: 2673-5490 doi:10.18429/JACoW-IPAC2021-THPAB056

CONCEPTUAL DESIGN OF A MULTIPLE PERIOD STAGGERED UNDULATOR

I. Asparuhov*, J. Chavanne, G. Le Bec
European Synchrotron Radiation Facility, Grenoble, France

Abstract

In staggered undulators, a ferromagnetic pole structure paired to a solenoid generates a sinusoidal field. Interest of such insertion devices has been studied for application to FEL systems in the end of the previous century. However, the concept has never been used in synchrotron radiation sources due to the undesirable magnetic effect of the solenoid on electron beam parameters in storage rings. Advent of fourth-generation low emittance light sources is foreseen to change this situation. Indeed, consequent electron beam transverse size and divergence reduction for such new storage rings give promise for a beam less sensitive to the presence of a longitudinal solenoidal field. Relating to this, a staggered concept can be an adequate design choice for short-period undulators producing high-energy photon flux. Such undulators would have a low K value *a priori* limiting their photon energy tunability. Considering integration of separate magnetic arrays of distinct periods in a solenoid to compose a global assembly can help suppress this possible drawback. Magnetic design and radiative performance of such an insertion device are presented.

INTRODUCTION

Typical peak field values attainable with the staggered technology are lower than those of corresponding permanent magnet devices at equal other comparative conditions (gap, period, etc.) [1, 2]. This effect is even more considerable for short periods and leads to a relatively small K value and hence low tunability through B_p at a given λ_p as can be seen in Eq. (1) [3]:

$$\lambda_{E_n} = \frac{\lambda_p}{2n\gamma^2}\left(1 + \frac{K^2}{2}\right). \quad (1)$$

Equation (1) gives the emitted on-axis radiation wavelength of the n-th harmonic λ_{E_n}, where γ is the relativistic Lorentz factor and $K \approx 0.0934 B_p[\mathrm{T}]\lambda_p[\mathrm{mm}]$ is the deflection parameter of the undulator.

To solve this issue one can think of ways to introduce new variation parameters for the harmonic energy. A pragmatic choice of such a parameter in a fixed-gap configuration for the staggered concept can be to implement period variation. Such an approach is presented for example in [4] where a single undulator array is mechanized for period length extension/reduction at a fixed number of periods N_p. In this paper a different scheme for the realization of period variability in a staggered design is proposed. It is based on an assembly composed of multiple fixed-period undulators of various $\lambda_p(n)$ and $N_p(n)$ totaling N in number where $n \in [0, N-1]$ (not to confuse with the harmonic number n in Eq. (1)). The arrays are positioned adjacently to one another at a distance d in the positive sens of the transverse horizontal direction Ox, in order of ascending $\lambda_p(n)$. In this manner a global period variation on the level of the assembly is achieved in the said direction along the pole width w_p of individual arrays. Figure 1 defines such an assembly in the form of a symmetric segment destined to be a unit building block for a longer assembly.

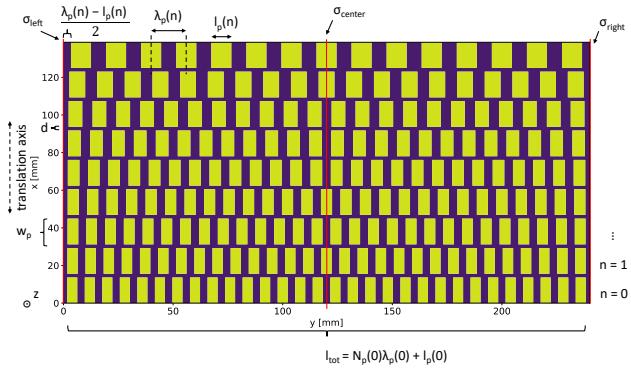

Figure 1: Top view of an upper-pole distribution of a symmetric (defined by the mid-plane σ_{center}) module made of $N = 9$ arrays. Mirror symmetry planes σ_{left} and σ_{right} would serve to adjoin identical neighbouring modules at either side of the array unit and thus demonstrate the modular aspect of the final global assembly.

The period range spans from 8 to 16 mm. This small-value interval extends below the rough lower boundary of periods readily accessible to more conventional undulator technologies like those based on permanent magnets. The latter are difficult to implement for $\lambda_p < 10$ mm, typically due to permanent magnet material brittleness for magnet blocks of resultingly small dimensions. The major part of current such designs have $\lambda_p \gtrapprox 14$ mm. Thus, the choice of a short-period design interval highlights and exploits a main relative practical interest of the staggered concept, another one being the absence of radiation damage experienced due to the lack of permanent magnets [4].

BASIC PHYSICAL AND OPERATING PRINCIPLE OF THE STAGGERED CONCEPT

Figure 2 defines the coordinate system used throughout the text and summarizes schematically the main design layout of a staggered undulator. An array of period λ_p and magnetic

* ilia.asparuhov@esrf.fr

ISBN: 978-3-95450-214-1 ISSN: 2673-5490 doi:10.18429/JACoW-IPAC2021-THPAB056

gap g made of magnetic poles of soft ferromagnetic material is placed inside a solenoid which is current-fed with a current density $\vec{j}$ to produce a solenoidal field $\vec{B}_{sol}$. This latter excites the staggered pole arrangement to give rise to a periodic vertical undulator field component B_z, of equal periodicity to that of the array geometry [2–8].

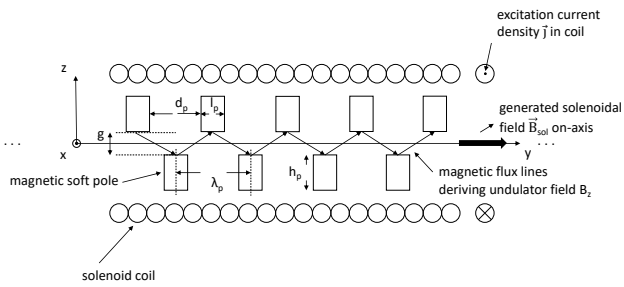

Figure 2: Sketch of a staggered undulator design showing a longitudinal cut of the basic components. The solenoid bore houses the arrangement of poles used to deflect the longitudinal solenoidal field to establish a periodic on-axis undulator field B_z in the gap g visualized by magnetic flux lines.

An approximate short-period analytical expression for the on-axis undulator peak field B_p, is given by [2,4,9]:

$$B_p = \frac{2B_s}{\sinh\left(\frac{\pi g}{\lambda_p}\right)}\left(\frac{\sin(\pi f)}{\pi f}\right). \qquad (2)$$

In Eq. (2) f is the ratio of pole spacing to undulator period (Fig. 2), $f = \frac{d_p}{\lambda_p}$, linked to the ratio $\alpha = \frac{l_p}{\lambda_p}$ of pole length l_p to period through $f = 1 - \alpha$, and B_s is the solenoid field at the center of the solenoid. Variation of B_s through j to act on B_p for other parameters fixed, namely gap g, is the main conceptual means to tune the harmonic energy of the emitted radiation in a staggered undulator [2,9], as alluded to by Eqs. (1) and (2).

SHORT-PERIOD MAGNETOSTATIC OPERATIONAL LIMITS

Table 1 presents results on optimized peak field B_p values and corresponding central solenoid field B_y for optimized pole width w_p =13.63 mm and longitudinal geometric ratio $\alpha \approx 0.57$ at different periods λ_p. Underlying calculations are done with the Radia 3D magnetostatic code [10] at a fixed magnetic gap $g = 4$ mm and pole height $h_p = 20$ mm. Simulative setup conditions are those of a pole array of $N_p = 20$, centered in the homogenous-field region of a solenoid of length $L_{sol} = 2.5\,\text{m} \gg N_p\lambda_p$ and radii $r_1 = 25$ mm, $r_2 = 30$ mm. A simple cylindrical model of a solenoid is used. Chosen pole material is 49Fe-49Co-2V Vanadium Permendur of saturation flux density B_{sat} = 2.3-2.4 T.

Table 1: Optimized Peak Field B_p Results with Corresponding Optimal Values of Solenoid Center Field for Integer Period Values in the Interval [8 mm, 16 mm]

λ_p[mm]	B_y[T]	B_p[T]
8	0.8724	0.4100
9	0.8400	0.4854
10	0.8206	0.5556
11	0.8136	0.6203
12	0.7710	0.6802
13	0.7502	0.7350
14	0.7304	0.7852
15	0.7082	0.8312
16	0.6954	0.8733

MAIN DESIGN CRITERIUM FOR CONTINUOUS ENERGY TUNABILITY

A particular period interval is ultimately determined by a dedicated parametrized design criterium. The latter is the functionally essential part of a valid set of main geometric specifications for an example module like the one shown in Fig. 1. The criterium reflects by construction magnetostatic results on staggered peak field operational limits obtained beforehand. It is derived from the setting of the requirement for continuity on the harmonic energy tunability interval in the case of the fundamental harmonic.

The considered perspective of period variation by switching among undulator arrays of different periods λ_p is practically realized through a corresponding discrete period increment value $\delta\lambda_p(n) = \lambda_p(n+1) - \lambda_p(n) > 0$ between neighbouring arrays. In such an operational scheme the aforementioned researched property of continuity for the energy variation interval translates into a necessary overlapping of individual array tuning curves in a more or less controlled manner. This would allow an expanded effective global *continuous* tuning range to be constituted for the assembly considered as a whole. In the hypothesis of independent magnetostatic operation of separate arrays one can formulate a design choice condition resulting in an interval of allowed switching step values $\delta\lambda_p(n)$ for each n. This is done in terms of a criterium function C depending on the corresponding period couple $(\lambda_p(n), \lambda_p(n+1))$:

$$\delta\lambda_p(n) \leq C(\gamma_{B_p}, \lambda_p(n), \lambda_p(n+1)) \qquad (3)$$

In Eq. (3) γ_{B_p} is assumed identical for all arrays and is defined by $B_{p\,min}(n) = \gamma_{B_p} B_{p\,max}(n)$ where $B_{p\,min}(n)$ is the lower boundary of the peak field variation range of array n and $B_{p\,max}(n)$ is the upper one, practically corresponding to the optimized value of $B_p(n)$. The function C in the case of the first harmonic λ_{E_1}, of prime interest to a staggered

ISBN: 978-3-95450-214-1 ISSN: 2673-5490 doi:10.18429/JACoW-IPAC2021-THPAB056

undulator, is precisely given by:

$$C(\gamma_{B_p}, \lambda_p(n), \lambda_p(n+1)) = \frac{e^2 B_0^2}{8\pi^2 m_{e0}^2 c^2} \times \left(\lambda_p^3(n) \exp\left(-\frac{2\pi g}{\lambda_p(n)}\right) - \gamma_{B_p}^2 \lambda_p^3(n+1) \exp\left(-\frac{2\pi g}{\lambda_p(n+1)}\right)\right) \quad (4)$$

In Eq. (4) B_0 [T] is an exponential gap-over-period fit constant over the period interval of interest, m_{e0} is the electron rest mass and c is the speed of light. Successive application of Eq. (3) and a straightforward geometric condition for the modular symmetry illustrated in Fig. 1 guarantees the strict inequality in Eq. (3) for all n.

Table 2: Resulting Individual Array $\lambda_p(n)$ and $N_p(n)$ for a Modular Assembly Yielded by the First Harmonic Energy Tunability Adjustment Criterium in the Period Interval [8 mm, 16 mm]

n	$\lambda_p(n)$[mm]	$N_p(n)$[1]
0	8	29
1	8.28	28
2	8.57	27
3	8.89	26
4	9.23	25
5	10	23
6	10.91	21
7	12.63	18
8	16	14

For initial parameter values $\gamma_{B_p} = 0.091$, $N = 9$, $\lambda_p(0) = 8$ mm, $N_p(0) = 29$, $B_0 = 1.9329$ T (calculated with the data in Table 1) the sequence of $\lambda_p(n)$ and $N_p(n)$ given in Table 2 is yielded.

Figure 3 shows on-axis tuning curves for flux and brilliance of the array module specified in Table 2 calculated with the SRW code [11]. The results are acquired for array lengths $L \approx 2$ m and the Extremely Brilliant Source (EBS) parameter beam given in Table 3 [12]. A resulting continuously covered global energy tuning range is observed with slight overlapping of the individual-array ranges illustrating a successful application of the specification method proposed.

Figure 4 shows corresponding power density plots for the minimal-period array of $\lambda_p(0) = 8$ mm from Table 2 for an array length $L \approx 2$ m taking into account a main field component $B_p = 0.3740$ T.

CONCLUSION

A basic conceptual approach for the specification of a continuously tunable variable-period modular undulator assembly of interest to staggered array designs is presented. Magnetostatic as well as radiative performance of such an assembly with an ultra-low horizontal emittance fourth-generation storage ring beam is investigated in respective terms of field optimization and flux, brilliance and power density. The study is focused on short undulator periods for improved first harmonic operation, reinforcing interest in the concept.

Table 3: Values for the EBS Beam in the Middle of a Straight Section

Parameter	Value	Unit
Average current I_{avg}	0.2	A
Energy E	6	GeV
Energy spread σ_E	0.00094	1
Horizontal emittance ϵ_x	132	pm.rad
Horizontal beta-function β_x	6.9	m
Horizontal dispersion function η_x	0.00173	1
Vertical emittance ϵ_z	5	pm.rad
Vertical beta-function β_z	2.64	m

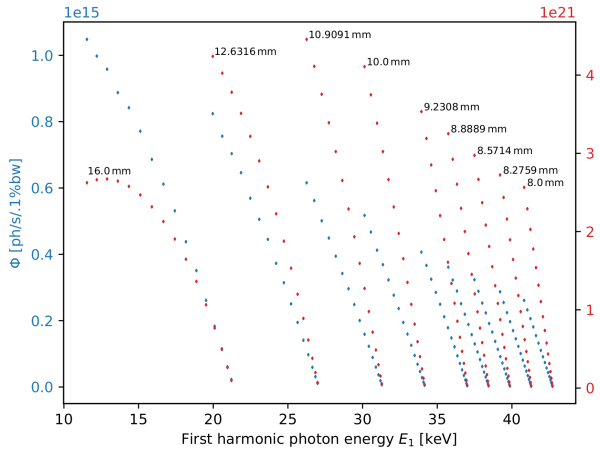

Figure 3: Tuning curves for flux (blue) and brilliance (red) produced on axis with the EBS-parameter beam indicated in Table 3 in the model frame of the first harmonic energy tunability adjustment criterium for the module array specifications of Table 2.

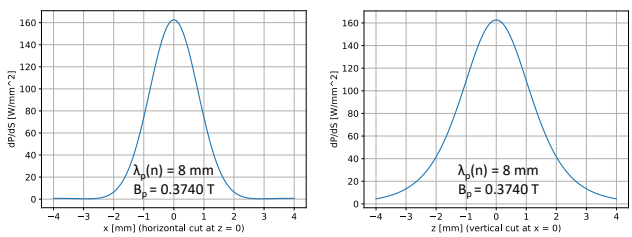

Figure 4: Projected transverse distribution profiles of power density at a distance $L_y = 30$ m from the source produced by array 0 of Table 2 ($\lambda_p(0) = 8$ mm, $B_p = 0.3740$ T) in the case of the EBS-parameter beam of Table 3.

REFERENCES

[1] S. Sasaki, "The possibility for a short-period hybrid staggered undulator", in *Proc. 2005 Particle Accelerator Conf. (PAC'05)*, Knoxville, Tennessee, USA, May 2005, paper RPAE005, pp. 982–984.

ISBN: 978-3-95450-214-1 ISSN: 2673-5490 doi:10.18429/JACoW-IPAC2021-THPAB056

[2] A. H. Ho, R. Pantell, J. Feinstein, and Y. Huang, "A Solenoid-Derived Wiggler", *IEEE J. Quantum Electron.*, vol. 27, no. 12, pp. 2650–2655, Dec. 1991. doi:10.1109/3.104145

[3] J. Chavanne, "Some undulator photon beam properties in a flat to round electron beam insertion", ESRF, Grenoble, France, Rep. 02-13/ID, Mar. 2013.

[4] G. K. Shenoy, J. W. Lewellen, D. Shu, and N. A. Vinokurov, "Variable-period undulators as synchrotron radiation sources", *J. Synchrotron Rad.*, vol. 10, pp. 205–213, 2003. doi:10.1107/S0909049502023257

[5] J. A. Pasour, F. Mako, and C. W. Roberson, "Electron drift in a linear magnetic wiggler with an axial guide field", *J. Appl. Phys.*, vol. 53, no. 11, pp. 7174–7178, Nov. 1982. doi:10.1063/1.331612

[6] K. Masuda *et al.*, "A design study of a staggered array undulator for high longitudinal uniformity of undulator peak fields by use of a 2-D code", *Nucl. Instr. Meth. A*, vol. 475, pp. 608-–612, 2001. doi:10.1016/S0168-9002(01)01583-2

[7] J. Kitagaki *et al.*, "A design study on electron beam confinement in a staggered array undulator based on a 3D code", *Nucl. Instr. Meth. A*, vol. 475, pp. 613-–616, 2001. doi:10.1016/s0168-9002(01)01582-0

[8] P. Brunelle *et al.*, "Application of an emittance adapter to increase photon flux density on a synchrotron radiation beam line", *Phys. Rev. Accel. Beams*, vol. 22, no. 6, p. 060702 , Jun. 2019. doi:10.1103/PhysRevAccelBeams.22.060702

[9] Y. C. Huang *et al.*, "Compact far-IR FEL design", *Nucl. Instr. Meth. A*, vol. 318, pp. 765–771, 1992. doi:10.1016/0168-9002(92)91155-3

[10] O. Chubar, P. Elleaume, and J. Chavanne, "A three-dimensional magnetostatics computer code for insertion devices", *J. Synchrotron Rad.*, vol. 5, pp. 481–484, 1998. doi:10.1107/S0909049597013502

[11] O. Chubar, P. Elleaume, "Accurate And Efficient Computation Of Synchrotron Radiation In The Near Field Region", in *Proc. 6th European Part. Accel. Conf (EPAC'98)*, Stockholm, Sweden, Jun. 1998, paper THP01G, pp. 1177-1179.

[12] S. M. White, "Commissioning and Restart of ESRF-EBS", presented at the 12th Int. Particle Accelerator Conf. (IPAC'21), Campinas, Brazil, May 2021, paper MOXA01, this conference.